

national accelerator laboratory

NAL-Pub-73/21-EXP

7200.037

UCLA-1071

(Submitted to Phys. Rev. Letters)

pp INTERACTIONS AT 303 GeV/c: INCLUSIVE STUDIES
OF γ , K_S^0 , AND Λ^0 PRODUCTION

F. T. Dao, D. Gordon, J. Lach, E. Malamud, and J. Schivell
National Accelerator Laboratory
Batavia, Illinois 60510

and

T. Meyer, R. Poster, P. E. Schlein, and W. E. Slater
University of California, Los Angeles
Los Angeles, California 90024

April 1973



pp INTERACTIONS AT 303 GeV/c: INCLUSIVE STUDIES
OF γ , K_S^0 , AND Λ^0 PRODUCTION

F. T. Dao, D. Gordon, J. Lach, E. Malamud, and J. Schivell
National Accelerator Laboratory
Batavia, Illinois 60510

and

T. Meyer, R. Poster, P. E. Schlein, and W. E. Slater*
University of California, Los Angeles
Los Angeles, California 90024

April 1973

ABSTRACT

We have studied the properties of the inclusive $pp \rightarrow \gamma X$, $K_S^0 X$, $\Lambda^0 X$, and $\bar{\Lambda}^0 X$ reactions in an exposure of the NAL 30-in. bubble chamber to a 303 GeV/c proton beam. From an analysis of V events observed in this experiment, we have obtained the following results: 1) the average number of particles produced per inelastic collision $\langle n_\gamma \rangle = 7.90 \pm 0.75$, $\langle n_{K_S^0} \rangle = 0.31 \pm 0.04$, $\langle n_{\Lambda^0} \rangle = 0.13 \pm 0.03$, and $\langle n_{\bar{\Lambda}^0} \rangle = 0.01 \pm 0.007$; 2) $\langle n_{\pi^0} \rangle$ rises approximately linearly with n_- implying that neutral and charged pions are strongly coupled, while $\langle n_{K_S^0} \rangle$ is less coupled to n_- ; 3) γ , K_S^0 , and Λ^0 production cross sections have reached a scaling limit by 303 GeV/c; and 4) $d\sigma/dy$ is relatively flat in the central region for K_S^0 and low multiplicity γ events.

* Supported by the United States National Science Foundation under grant GP-33565.

In this letter we report on our study of V^0 events from an exposure of 303 GeV/c protons in the 30-inch hydrogen bubble chamber at the National Accelerator Laboratory. Results on multiplicity, total cross section, and inclusive Δ^{++} production have already been reported.¹ A total of 311 V^0 events were recorded in a fixed fiducial volume.² These events were processed through TVGP and SQUAW and fitted to the following hypotheses: $K_S^0 \rightarrow \pi^+ \pi^-$, $\Lambda^0 \rightarrow p \pi^-$, $\bar{\Lambda}^0 \rightarrow \pi^+ \bar{p}$ and $\gamma(p) \rightarrow e^+ e^-(p)$. After two measurements, 71% of the 311 events had satisfactory fits, 19% did not point to the primary vertex, and 10% were unmeasurable. The events were examined on a scan table by physicists. Of the 311 fitted events, 18% had more than one satisfactory fit. A selection on the transverse momentum of the negative outgoing track with respect to the neutral particle³ was effective in resolving all the γ ambiguities. The small number of K_S^0/Λ^0 ambiguities was resolved by ionization and χ^2 . These were edited on the scan table using ionization information.

After all selections there were 119 γ , 50 K_S^0 , 20 Λ^0 , and 2 unique $\bar{\Lambda}^0$.⁴ The data for K_S^0 , Λ^0 , and $\bar{\Lambda}^0$ were restricted to the backward hemisphere in the pp center of mass as the detection efficiency in the forward direction was extremely low. The average weighting factors⁵ are: 71.9 for γ , 3.44 for K_S^0 , 4.25 for Λ^0 , and 4.69 for $\bar{\Lambda}^0$. The final sample was further corrected by a scanning efficiency of 0.93. The inclusive cross sections measured (that is, the product of the average

number of particles produced per inelastic collision and the total inelastic cross section) are: $\sigma(\gamma) = 253 \pm 24$ mb, $\sigma(K_S^0) = 9.8 \pm 1.3$ mb, $\sigma(\Lambda^0) = 4.2 \pm 1.0$ mb and $\sigma(\bar{\Lambda}^0) = 0.4 \pm \begin{matrix} 1.0 \\ 0.3 \end{matrix}$ mb. Assuming that all γ 's come from $\pi^0 \rightarrow 2\gamma$, we get $\sigma(\pi^0) = (127 \pm 12)$ mb.

The dependencies of these cross sections on the incident laboratory momentum^{6, 7, 8, 9} are shown in Figs. 1(a), (b), and (c). Note that $\sigma(\Lambda^0)$ has increased threefold from 28 GeV/c to 303 GeV/c and remains much larger than $\sigma(\bar{\Lambda}^0)$ at 303 GeV/c. The K_S^0 cross section has increased more than eight times from 28 GeV/c to 303 GeV/c. However, the rapid rise in $\sigma(K_S^0)$ may level off at energies beyond 303 GeV/c as indicated by the ISR data.¹⁰ The π^0 cross section in Fig. 1(c) is consistent with a logarithmic growth with incident momentum and is equal to $\sigma(n_-)$ or $\sigma(\pi^-)$ if we assume all negatively charged particles to be π^- 's. This is in accord with multiperipheral models that predict $\langle n_{\pi^0} \rangle = \langle n_{\pi^-} \rangle = \langle n_{\pi^+} \rangle$,¹¹ where $\langle n_x \rangle$ is the average number of particles of type x produced per inelastic pp collision.

The topological cross sections and $\langle n_{\pi^0} \rangle$ and $\langle n_{K_S^0} \rangle$ vs topology for inclusive π^0 and K_S^0 production are listed in Table I.

In Fig. 2(a) and (b) $\langle n_{\pi^0} \rangle$ and $\langle n_{K_S^0} \rangle$ are plotted as a function of charged multiplicity, n_c . Two possible dependencies are shown:

$\langle n_{K_S^0} \rangle = 0.31$ assumes K_S^0 production is independent of topology;

$\langle n_{K_S^0} \rangle = 0.09 n_-$ is based on $\sigma_{K_S^0} / \sigma_{\pi^-}$ being independent of topology.

In contrast $\langle n_{\pi^0} \rangle$ tends to rise linearly with n_c for $n_c \leq 18$. The

latter linear dependence which has been observed here and earlier at 205 GeV/c is very different from the low energy pp data.¹² The broken straight line in Fig. 2(b) is given by $\langle n_{\pi^0} \rangle = n_-$. If we assume all the negative particles to be pions, the data imply that the isospin states of the pion are strongly correlated. Berger, Horn and Thomas¹³ conclude that a linear rise of $\langle n_{\pi^0} \rangle$ versus n_c at high energies rules out models in which pions are independently emitted but is in accord with fragmentation models and multiperipheral models in which ρ or ω type meson clusters are emitted. The weaker dependence of $\langle n_{K_S^0} \rangle$ on n_c may reflect the lack of strong correlation between kaons and pions.

In Figs. 3(a) and (b), we show the invariant single particle distribution in Feynman variable x for the inclusive K_S^0 and Λ^0 reactions. Our results combined with the 205 GeV/c data⁷ give evidence that the inclusive K_S^0 and Λ^0 reactions have reached their scaling limits from below, with Λ^0 approaching the limit at a much faster rate than K_S^0 .

Figures 4(a) and (b) show $d\sigma/dy$ versus the rapidity variable y for the K_S^0 and γ reactions. There is evidence for a plateau with widths of two units in y for the K_S^0 and low multiplicity γ events; $d\sigma/dy$ seems to peak at $y = 0$ for high multiplicity γ events. The average longitudinal momentum in the center of mass $\langle |p_L| \rangle = 2.90 \pm 0.56$, 1.11 ± 0.17 , and 0.88 ± 0.12 GeV/c for Λ^0 , K_S^0 , and π^0 respectively.¹⁴ Thus, neutral pions and kaons are produced more frequently in the central region than Λ^0 's.

We acknowledge the support of the NAL accelerator and neutrino area operations staffs and the 30-inch bubble chamber group during the run, and the dedicated work of the staff of the NAL film analysis facility in analyzing the data.

References

¹P. T. Dao et al., Phys. Rev. Letters 29, 1627 (1972).

P. T. Dao et al., Phys. Rev. Letters 30, 34 (1973).

²The fiducial volume for the primary interaction vertex was chosen to be smaller than the ones mentioned in Ref. 1 to allow enough track length for decay or conversion. The fiducial volume for the V^0 vertex was defined as $(x_v - 3)^2 + y_v^2 \leq (28 \text{ cm})^2$ and $0 \leq z_v \leq 37.72 \text{ cm}$, where (x_v, y_v, z_v) are spatial coordinates for the V^0 vertex.

³The following cuts on the transverse momentum p_T in MeV/c were made: $0 \leq p_T \leq 15$ for γ , $15 \leq p_T \leq 210$ for K_S^0 , and $15 \leq p_T \leq 105$ for Λ^0 and $\bar{\Lambda}^0$.

Note that these cuts are equivalent to making a very small cut (0.3%) in the $\cos\theta$ distribution in the center of mass of K_S^0 , Λ^0 , and $\bar{\Lambda}^0$ decays.

⁴Ten $\bar{\Lambda}^0 \rightarrow \bar{p}\pi^+$ candidates were found and edited on the scan table using ionization information. The result was: 2 unique $\bar{\Lambda}^0$, 3 unique K_S^0 , and 5 events that fit $\bar{\Lambda}$ and at least one other hypothesis (usually K_S^0).

⁵Each event was weighted by a factor calculated from the potential decay length and neutral decay branching ratio. The minimum length for efficient detection was 4 cm for γ and 2 cm for K_S^0 , Λ^0 , and $\bar{\Lambda}^0$. The pair conversion cross section for γ was calculated by T. M. Knasel, DESY Reports Nos. 70/2 and 70/3.

⁶B. Y. Oh and G. A. Smith, "Inclusive Study of Λ^0 and Σ^\pm Hyperons Produced in Proton-Proton Collisions from 6.6 to 28 GeV/c", paper

submitted to XVI International Conference on High Energy Physics, Batavia (1972).

⁷G. Charlton et al., Phys. Rev. Letters 30, 574 (1973).

⁸G. Charlton et al., Phys. Rev. Letters 29, 1759 (1972).

⁹G. Neuhofer et al., Phys. Letters 38B, 51 (1972); and Phys. Letters 37B, 438 (1971).

¹⁰The ISR data points in Fig. 1(b) were computed on the assumption that neutral kaon emission is as frequent as charged kaon emission. Thus,

$$\sigma(K_S^0) = \left(\frac{R\left(\frac{K^+}{\pi^+}\right) + R\left(\frac{K^-}{\pi^-}\right) R\left(\frac{\pi^-}{\pi^+}\right)}{1 + R\left(\frac{\pi^-}{\pi^+}\right)} \right) \sigma(\pi^0)$$

where the ratios were obtained from A. Bertin et al., Phys. Letters 41B, 201 (1972) and the π^0 cross section from Ref. 9.

¹¹J. Honerkamp and K. H. Mütter, Nucl. Phys. B38, 565 (1972).

¹²H. Boggild et al., Nucl. Phys. B27, 285 (1971).

¹³E. L. Berger, D. Horn, and G. H. Thomas, ANL/HEP Report 7240 (1972).

¹⁴G. I. Kopylov, Nucl. Phys. B52, 126 (1973), derives $\langle p_L(\pi^0) \rangle = 2 \langle p_L(\gamma) \rangle$.

¹⁵H. J. Mück et al., Phys. Letters 39B, 303 (1972).

TABLE I
 Cross Sections for $pp \rightarrow \pi^0 X$ and $K_S^0 X$

n = Number of Charged Particles	$\sigma_n(pp \rightarrow \pi^0 X)^*$ in mb	$\langle n_{\pi^0} \rangle$	$\sigma_n(pp \rightarrow K_S^0 X)$ in mb	$\langle n_{K_S^0} \rangle$
2	1.7 ± 1.2	1.0 ± 0.7	0.2 ± 0.2	0.1 ± 0.1
4	11.8 ± 3.1	2.4 ± 0.7	0.8 ± 0.4	0.2 ± 0.1
6	19.4 ± 4.1	3.4 ± 0.8	2.9 ± 0.7	0.5 ± 0.1
8	16.0 ± 3.7	3.0 ± 0.7	1.4 ± 0.5	0.3 ± 0.1
10	22.8 ± 4.4	4.8 ± 1.0	1.6 ± 0.5	0.4 ± 0.1
12	20.3 ± 4.1	4.8 ± 1.4	1.3 ± 0.4	0.3 ± 0.1
14	15.7 ± 2.5	7.2 ± 1.5	0.6 ± 0.2	0.3 ± 0.1
16	9.3 ± 2.8	6.7 ± 2.2	0.8 ± 0.4	0.6 ± 0.3
18	7.2 ± 2.5	8.3 ± 3.2	---	---
20	1.6 ± 1.1	3.3 ± 2.4	0.2 ± 0.2	0.3 ± 0.3
22	---	---	---	---
24	---	---	---	---
26	0.9 ± 0.9	17.0 ± 17.0	---	---
TOTAL	126.7 ± 12.0	3.95 ± 0.38	9.8 ± 1.3	0.31 ± 0.04

* Calculated from $\sigma_n(pp \rightarrow \pi^0 X) = \sigma_n(pp \rightarrow \gamma X)/2$.

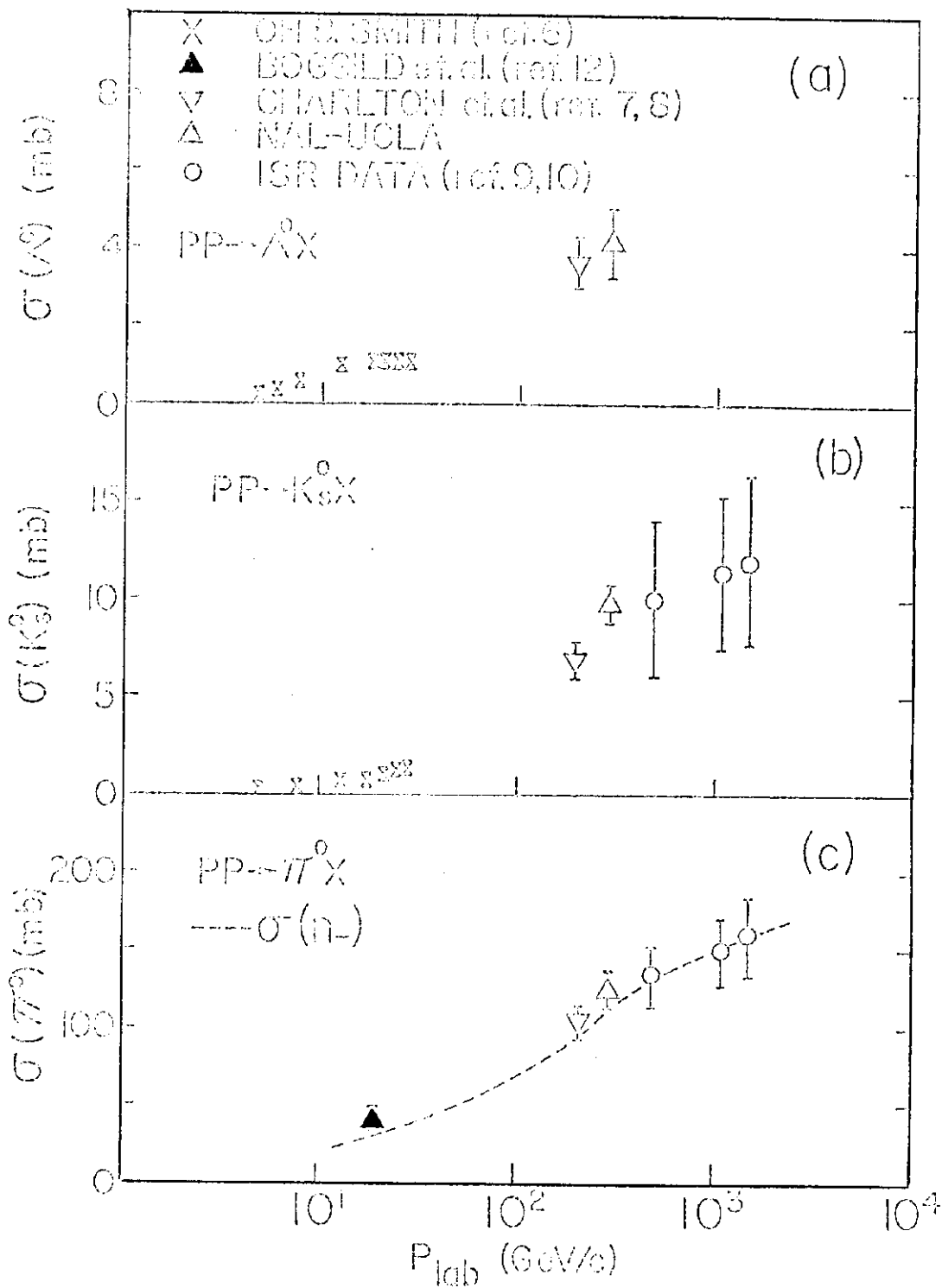


Fig. 1 (a) $\sigma(pp \rightarrow \Lambda^0 X)$, (b) $\sigma(pp \rightarrow K_S^0 X)$, and (c) $\sigma(pp \rightarrow \pi^0 X)$ versus incident laboratory momentum P_{lab} . See Ref. 10 for derivation of data points beyond 303 GeV/c.

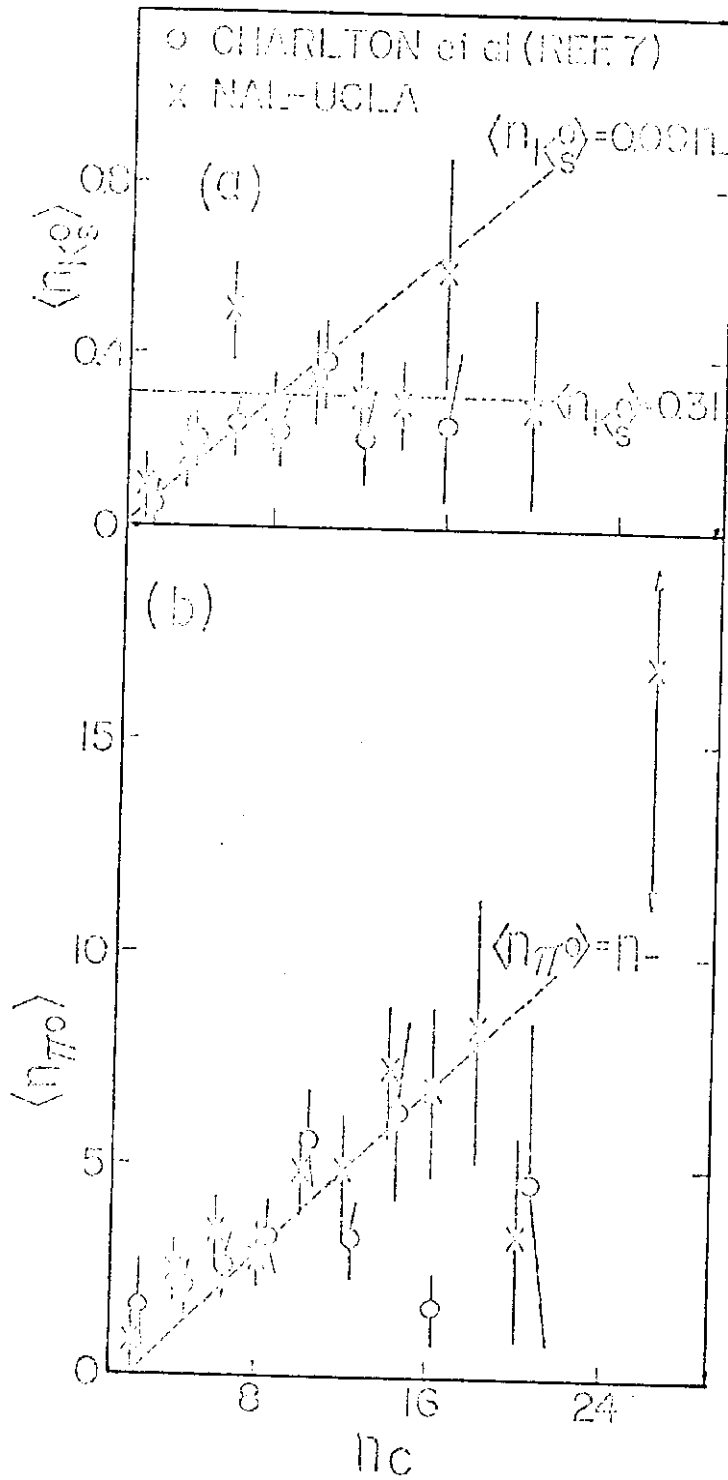


Fig. 2 (a) Average number of K_S^0 and (b) average number of π^0 's produced per inelastic pp collision versus charged multiplicity. The curves are described in the text.

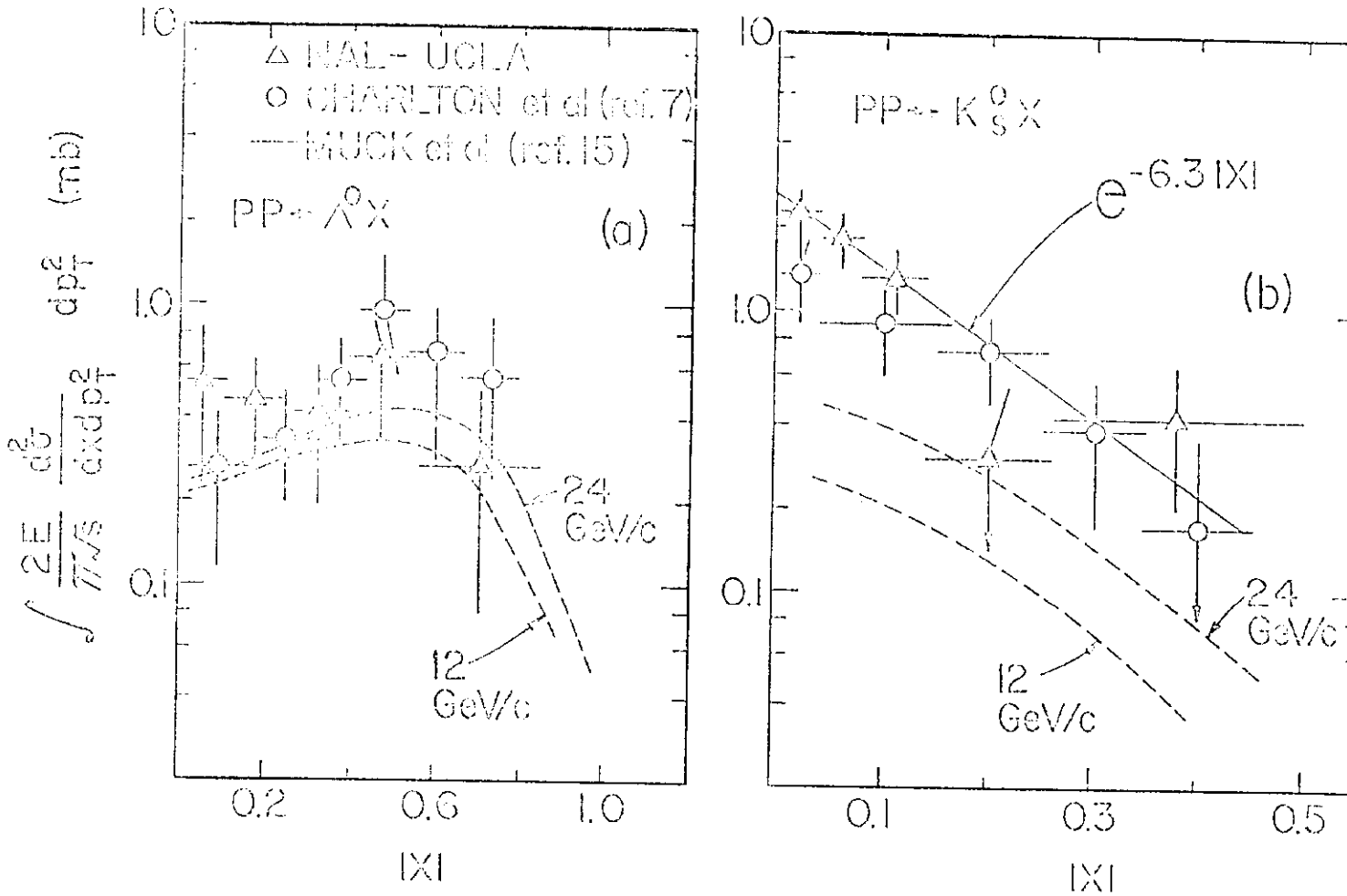


Fig. 3 Invariant distribution

$$\int \frac{2E}{\pi \sqrt{s}} \frac{d^2\sigma}{dx dp_T^2} dp_T^2$$

versus $|x|$ for (a) $pp \rightarrow \Lambda^0 X$

and (b) $pp \rightarrow K_S^0 X$,

and E , p_T , and p_L are the energy, transverse, and

longitudinal momentum of the particle in the center of mass

and $x = 2 p_L / \sqrt{s}$.

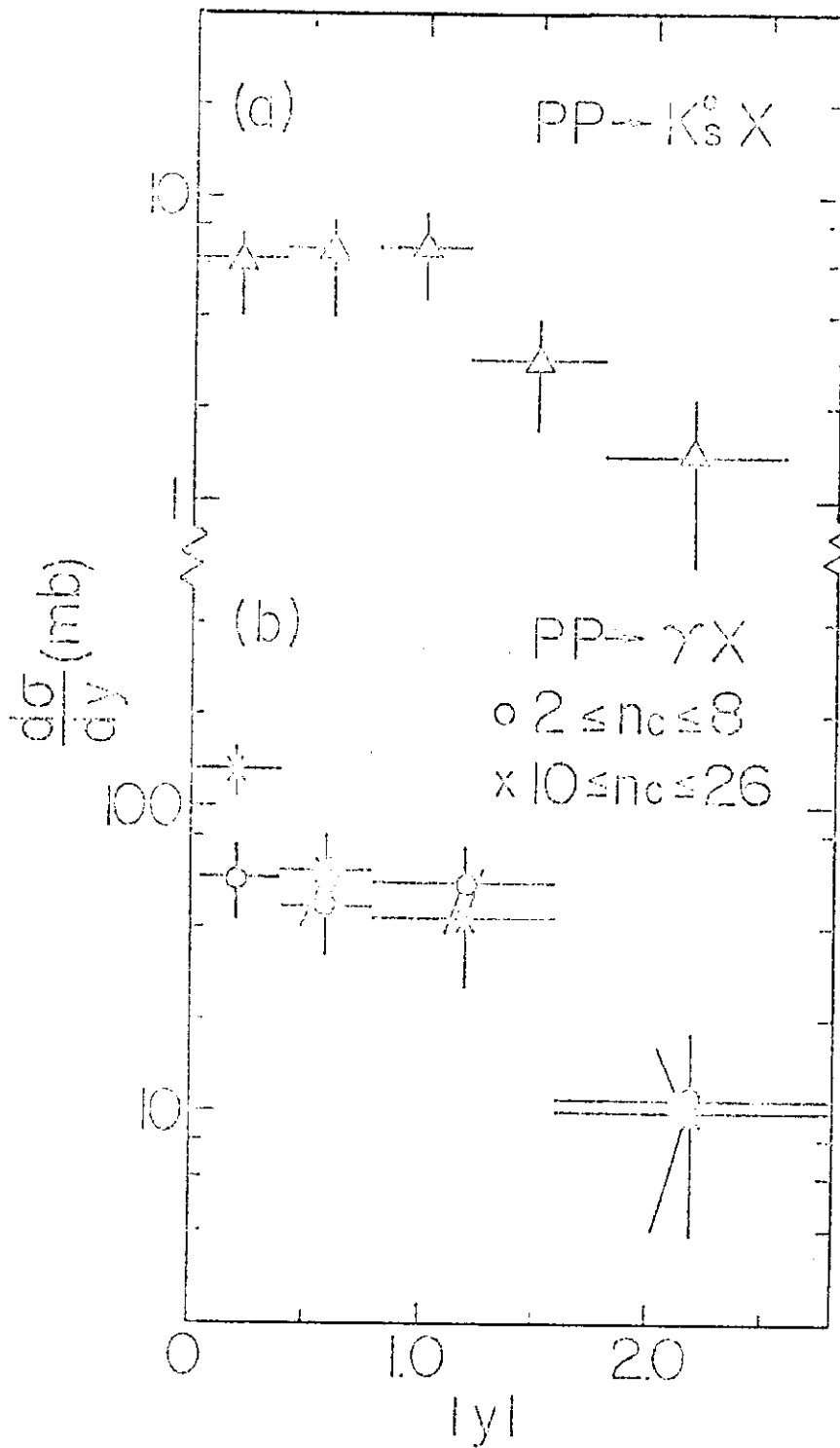


Fig. 4 $d\sigma/dy$ versus y for (a) $pp \rightarrow K_S^0 X$ and (b) $pp \rightarrow \gamma X$.